Discrete elliptic solitons in two-dimensional waveguide arrays

Fangwei Ye (叶芳伟), Liangwei Dong (董亮伟), Jiandong Wang (王建东), Tian Cai (蔡 田), and Yong-Ping Li (李永平)

Department of Physics, University of Science and Technology of China, Hefei 230026

Received September 14, 2004

The fundamental properties of discrete elliptic solitons (DESs) in the two-dimensional waveguide arrays were studied. The DESs show nontrivial spatial structures in their parameters space due to the introduction of the new freedom of ellipticity, and their stability is closely linked to their propagation directions in the transverse plane.

OCIS codes: 190.5530, 190.3100, 190.4370, 060.5530.

Discrete spatial solitons in nonlinear lattices have been received considerable attention in many branches of science[1]. They have been demonstrated to exist in a wide range of physical systems such as biological molecules[2], solid-state systems[3], Bose-Einstein condensate[4], and nonlinear optical waveguide[5,6]. The underlying dynamics in these systems is dominated by the competition of the couplings between the adjacent potential wells and nonlinearity. A balance between these two effects can result in a self-localization state: discrete soliton (DS). DSs in optics were firstly predicted in nonlinear waveguide arrays in 1988[5], and were successfully observed a decade later[7]. It differs fundamentally from their bulk counterpart in several aspects[8]. For example, a unique property that origins from the discrete nature of the waveguide is that of reverse diffraction; this leads to the diffraction management[9] and the observation of the dark soliton in self-focusing Kerr media.

The previous studies on DS have been limited primarily to the one-dimensional (1D) waveguide array, and recent years witnessed a shift of interest to the higher dimensions both on theories and experiments[10−14]. This is because that many exciting and new DS features can only occur in the higher dimensions, and the two-dimensional (2D) waveguide arrays are considerably more complex and versatile than their 1D counterpart. One of the most interesting entities in the 2D environments is DS carrying orbital angular momentum or discrete (lattice) vortex solitons[12−17]. The discrete vortex solitons that are suggested theoretically can be supported by the lattice even in the self-focusing region, and have been demonstrated experimentally in the isotropic photorefractive nonlinear media[12,13].

Our work was stimulated by Ref. [11], where the authors predicted the existence of a new class of solitons in the 2D square waveguide arrays, namely, discrete elliptic solitons (DESs), which is due to the anisotropic diffraction in the high-dimensional systems. DESs are moving solitons that travel across the array in order to get the different diffraction strengths in the x and y directions.

In this letter, we studied further the fundamental properties of these DESs, especially their spatial structure and stability. We would like to mention that our study object in this letter is the same as that in the Ref. [11], however, our study here revealed two new interesting results on DESs. Firstly, we demonstrated the unique difference of DESs from those stationary solitons[17−19] in their parameter space due to the introduction of the new freedom of ellipticity. Secondly, by numerous numerical experiments, we revealed that the stability of DESs is closely linked to their moving directions in the transverse plane, and found that there are just several special directions which support the stable DESs. Besides these two points, we also put forward a new scheme to determine the coupling coefficients in the periodic system. This scheme is more physical and convenient than the usual method to determine the coupling coefficients by the direct computing formula[17,18].

As shown in Ref. [11], we also consider the evolution of the beam envelope in the 2D waveguide array. The linear refraction index is $n = n_0 + f(x, y)$, where n_0 is the index of the background, $f(x, y)$ represents refractive-index distribution of the 2D waveguide array as sketched in Fig. 1. Mathematically, $f = \delta \sum_{m,n} \mathrm{circ}(\frac{x-md}{a}, \frac{y-nd}{a})$, where $\mathrm{circ}(\frac{r}{a})$ equals unity for $r \le a$ and 0 otherwise, δ is its amplitude. We also assumed a saturable nonlinearity with saturable intensity I_s of $\Delta n(|u|^2) = \frac{I_s|u|^2}{I_s+|u|^2}$. The paraxial evolution now is given by[11−13]

$$i\frac{\partial u}{\partial z} + \frac{1}{2k}\nabla_\perp^2 u + \frac{k}{n_0} f(x, y)u + \frac{kn_2}{n_0}\frac{I_s|u|^2}{I_s + |u|^2}u = 0. \quad (1)$$

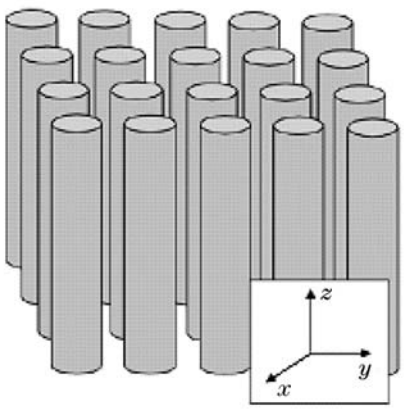

Fig. 1. A 2D waveguide array. Cladding index $n_0 = 1.5$, waveguide index $n_c = 1.5003$, lattice constant $d = 15.9$ μm, radius of the waveguide $a = 5.3$ μm, assume the operating wavelength is 1.5 μm.

Our aim was to find the solutions of DESs to Eq. (1). However, it is very troublesome to tackle with this original equation, much less the clear physical significance. Fortunately, the high mode localization in each waveguide validates the tightly-binding approximation[17,18] and allows the decomposition of the wavefunction into a sum of local modes, $\phi_{m,n}(x,y)$, as

$$u = \sum_{m,n} c_{m,n}(z)\phi_{m,n}(x,y). \tag{2}$$

Replacing Eq. (2) into Eq. (1), we obtained a set of the normalized discrete nonlinear Schrödinger equations (DNLSE)

$$\begin{aligned} &i\frac{\mathrm{d}c_{m,n}}{\mathrm{d}z} + \kappa(c_{m-1,n} + c_{m+1,n} + c_{m,n-1} + c_{m,n+1}) \\ &+\tau(c_{m-1,n-1} + c_{m+1,n-1} + c_{m-1,n+1} + c_{m+1,n+1}) \\ &+\frac{|c_{m,n}|^2}{1+|c_{m,n}|^2}c_{m,n} = 0, \end{aligned} \tag{3}$$

where κ and τ are the coupling coefficients of nearest-neighbor and next-nearest-neighbor, given by $\kappa = \langle\phi_{m,n}|[f - \mathrm{circ}(\frac{r}{a})]|\phi_{m,n+1}\rangle$ and $\tau = \langle\phi_{m,n}|[f - \mathrm{circ}(\frac{r}{a})]|\phi_{m+1,n+1}\rangle$, respectively ($\langle\rangle$ is Dirac integration sign). However, we found it is more convenient and effective to find these coupling coefficients numerically by performing a beam propagation method (BPM)[20] simulation of a directional coupler. Under the parameters given in Fig. 1, the numerical method gave out the values of the two coupling coefficients $\kappa = 277\ \mathrm{m}^{-1}$, and $\tau = 45\ \mathrm{m}^{-1}$, which agree well with the result from direct computing formula as in the previous publications[17,18].

We considered here the moderately confined DESs, therefore, the so-called long-wave approximation[5,6] can be employed. Writing $c_{m,n} = E_{m,n}\exp\{i(mp+nq) + i[2\kappa(\cos(p)+\cos(q)) + 4\tau\cos(p)\cos(q)]\}$ and $E_{m,n\pm1} = \Phi - d\Phi_y + (\frac{d^2}{2})\Phi_{yy}$, and then executing a coordinate translation and rotational operators, Eq. (3) is turned into

$$i\psi_z + \varepsilon\psi_{uu} + \mu\psi_{vv} + \frac{|\psi|^2}{1+|\psi|^2}\psi = 0, \tag{4}$$

where $\mu = \alpha\sin^2(\theta) + \beta\cos^2(\theta) - \gamma\cos(\theta)\sin(\theta)$, $\epsilon = \alpha\cos^2(\theta) + \beta\sin^2(\theta) + \gamma\cos(\theta)\sin(\theta)$, $\alpha = \kappa d^2\cos(p) + 2\tau d^2\cos(p)\cos(q)$, $\beta = \kappa d^2\cos(q) + 2\tau d^2\cos(p)\cos(q)$, $\gamma = -4\tau d^2\sin(p)\sin(q)$, and $\theta = \frac{1}{2}\tanh^{-1}(\frac{4\tau\sin(p)\sin(q)}{\cos(p)-\cos(q)})$ (see Ref. [11] for more details about the coordinate transformations).

Lastly under a coordinate rescaling: $x' = \frac{1}{\sqrt{\varepsilon}}u$, $y' = \frac{1}{\sqrt{\mu}}v$, Eq. (4) is transformed into a more familiar style which can be solved readily in the cylindrical coordinates,

$$iE_z + \nabla_\perp^2 E + \frac{|E|^2}{1+|E|^2}E = 0. \tag{5}$$

The quantity E in Eq. (5) (or ψ in Eq. (4)) should be understood as the envelope containing the discrete fields $c_{m,n}$. After obtaining the soliton's envelope solution by substituting $E(x,y,z) = \Phi(x,y)\exp(i\lambda z)$ into Eq. (5) ($\lambda = 0.5$ is the soliton's nonlinear propagation constant), we recovered the desired soliton solutions of the original equation (Eq. (1)) by a series of the anti-transformations (reverse to the transformations as described above).

Figures 2(a)—(d) depicted four typical DESs with the same nonlinear propagation constant ($\lambda = 0.5$) but with different values of p and q. As shown in Fig. 2, (p,q) values determine the amount of ellipticity of the DESs, as well as their orientation of principal axes. The DESs with the same nonlinear propagation constant and different ellipticities have different powers P ($P = \int\int |u(x,y)|^2\mathrm{d}x\mathrm{d}y$) (see Fig. 3). Note that the DESs depicted here all belong to the lowest-order soliton family since they are all single-humped (the readers should not be confused with the spatially modulated envelope of the DES due to the periodic modulation of the refractive index). Such power features of DESs are much different from that of stationary gap solitons[17–19], where the different powers originate from the nonlinear eigenmodes with different orders hence different number of humps. The most interesting case of these DESs maybe is those whose ellipticities locate between the bands, i.e., $p = q = \frac{\pi}{2}$, where the effective diffraction is nearly zero[9]. Therefore, they are of the narrowest spatial width and require the lowest power to be excited. These special kinds of DESs are now under our study and the results will be published elsewhere.

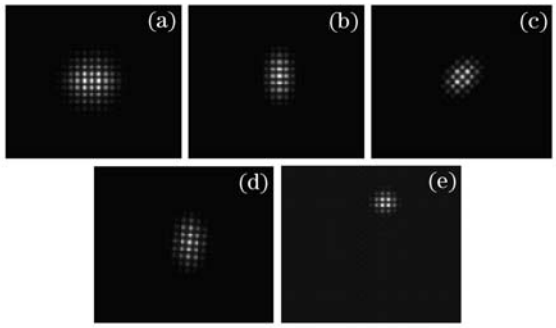

Fig. 2. Spatial intensity distribution of DES with nonlinear propagation constant $\lambda = 0.5$. (a) $p = 0$, $q = 0$; (b) $p = 0$, $q = 1.0$ (0 deg. DES); (c) $p = 1.0$, $q = 1.0$ (45 deg. DES); (d) $p = 0.2$, $q = 1.2$ (80 deg. DES); (e) The initial elliptic soliton (Fig. 2(d)) redistributes itself into a more circular shape during propagation ($z = 2.5$ cm).

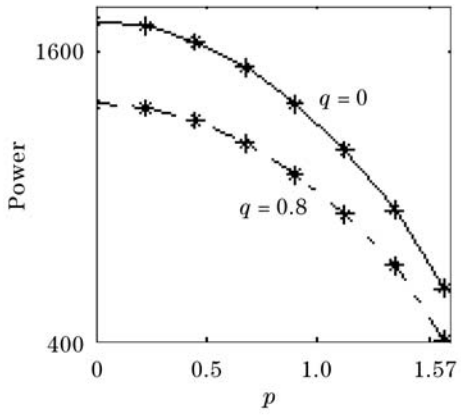

Fig. 3. Two typical power curves which correspond to the same nonlinear propagation constant $\lambda = 0.5$.

The stability of soliton is very important since only those stable solitons are possibly observed in experiments. We have performed a series of numerical simulation to test the stability of DESs. Our scheme is to use the soliton solution obtained above as input in Eq. (1), then using a BPM technique to propagate it. We found in the numerous simulations that, for the 0 deg. ($p \neq 0$, $q = 0$) (or 90 deg. ($p = 0$, $q \neq 0$)) soliton, it propagates in the x (or y) axis direction very robustly indicating the formation of a stable DES. A very similar phenomenon is seen in the numerical simulation for DES with 45 deg. ($p = q \neq 0$). At this angle, the soliton lays its principal axes along the bisector of the angle made by x and y axis, and shows a very robust propagation along that direction. Nevertheless, for any other angles, the input DES seems like to evolve into a something which is more circular, therefore, unstable. A typical example of the unstable evolution of these DESs is shown in Figs. 2(d) and (e). Figure 2(e) shows the intensity distribution of an 80 deg. DES at propagation distance $z = 2.5$ cm, while Fig. 2(d) shows its initial distribution. This DES can be clearly observed the deviation from the initial elliptic intensity distribution (see Fig. 2(d)) and collapse into a circular distribution. Comparing with these simulation results, it is concluded that, at angles such as 0, 45, and 90 deg., the moving DESs "feel" a periodic refractive index distribution therefore fairly stable; however, at any other angles, they are perturbed by a random refractive index variation then gradually lose the original preponderant directions and turn themselves into isotropic entities. Therefore, at these angles, an original elliptic soliton turns into a circular one. Notice that, the unstable evolvement from ellipse to circle is in sharp contrast with the well-known symmetry breaking instability, which always leads a symmetrical soliton evolve into an asymmetry one.

In conclusion, we studied the spatial structure and stability of DESs in the 2D periodic system. Due to the introduction of the new freedom of ellipticity, these DESs show nontrivial spatial structure properties in their parameter space. The stability of DESs depends crucially on their propagation directions in the transverse plane, and only some specific directions support stable DESs.

This work was supported by the National Natural Science Foundation of China under Grant No. 10274078. F. Ye thanks helpful discussion with Jared Hudock. F. Ye's email address is fwye@ustc.edu.

References

1. A. Scott, Phys. Rep. **217,** 1 (1992).
2. A. S. Davydov and N. I. Kislukha, Phys. Status Solidi B **59,** 465 (1973).
3. W. P. Su, J. R. Schrieffer, and A. J. Heeger, Phys. Rev. Lett. **42,** 1698 (1979).
4. A. Trombettoni and A. Smerzi, Phys. Rev. Lett. **86,** 2353 (2001).
5. D. N. Christodoulides and R. I. Joseph, Opt. Lett. **13,** 794 (1988).
6. X. Gu, X. Chen, Y. Chen, Y. Xia, and Y. Chen, Chin. Opt. Lett. **1,** 671 (2003).
7. H. S. Eisenberg, Y. Silberberg, R. Morandotti, A. R. Boyd, and J. S. Aitchison, Phys. Rev. Lett. **81,** 3383 (1998).
8. D. N. Christodoulides, F. Lederer, and Y. Siberberg, Nature **424,** 817 (2003).
9. H. S. Eisenberg, Y. Silberberg, R. Morandotti, and J. S. Aitchison, Phys. Rev. Lett. **85,** 1863 (2000).
10. T. Pertsch, U. Peschel, F. Lederer, J. Burghoff, M. Will, S. Nolte, and A. Tünnermann, Opt. Lett. **29,** 468 (2004).
11. J. Hudock, N. K. Efremidis, and D. N. Christodoulides, Opt. Lett. **29,** 268 (2004).
12. D. N. Neshev, T. J. Alexander, E. A. Ostrovskaya, Y. S. Kivshar, H. Martin, I. Makasyuk, and Z. Chen, Phys. Rev. Lett. **92,** 123903 (2004).
13. Z. Chen, H. Martin, E. D. Eugenieva, J. Xu, and A. Bezryadina, Phys. Rev. Lett. **92,** 143902 (2004).
14. J. W. Fleischer, M. Segev, N. K. Efremidis, and D. N. Christodoulides, Nature **422,** 147 (2003).
15. F. Ye, J. Wang, L. Dong, and Y.-P. Li, Opt. Commun. **230,** 219 (2004).
16. L. Dong, F. Ye, J. Wang, T. Cai, and Y.-P. Li, Physica D **194,** 219 (2004).
17. A. Trombettoni and A. Smerzi, Phys. Rev. Lett. **86,** 2353 (2001).
18. N. K. Efremidis and D. N. Christodoulides, Phys. Rev. A **67,** 063608 (2003).
19. P. J. Y. Louis, E. A. Ostrovskaya, C. M. Savage, and Y. S. Kivshar, Phys. Rev. A **67,** 013602 (2003).
20. M. D. Feit and J. A. Fleck, Appl. Opt. **17,** 3990 (1978).